

Toughness improvement of epoxy thermosets with cellulose nanocrystals

Xiulian Qin, Wenming Ge, Honggang Mei, Lei Li* and Sixun Zheng*



Abstract

We report the toughness improvement of epoxy thermosets by the use of cellulose nanocrystals (CNCs). Pristine CNCs were functionalized via surface-initiated reversible addition–fragmentation chain transfer/macromolecular design via interchange of xanthates (RAFT/MADIX) polymerization. The pristine CNCs were first surface-treated with 4-cyano-4-(isopropoxycarbonylthio)pentanoic chloride and then poly(*N*-vinylpyrrolidone)-grafted CNCs (CNC-PVPy) were synthesized with the xanthate-functionalized CNCs as chain transfer agent. Notably, the as-obtained CNC-PVPy can be dispersed into epoxy thermosets in the form of single fibrous nano-objects, i.e. the nanocomposites of epoxy with CNCs were successfully obtained. The uniform dispersion of CNCs in epoxy matrix is attributable to the compatibilizing effect of PVPy chains. The introduction of CNCs markedly improved the toughness of epoxy thermosets. When the mass fraction of CNC-PVPy was 30 wt%, the nanocomposites displayed the maximum critical stress intensity factor (K_{1c}) and critical fracture energy (G_{1c}) of $1.76 \text{ MN m}^{-3/2}$ and 0.66 kJ m^{-2} , respectively. The toughening of epoxy thermosets is mainly attributed to the plastic deformation of epoxy matrix, which is initiated from CNCs.

© 2021 Society of Industrial Chemistry.

Supporting information may be found in the online version of this article.

Keywords: cellulose nanocrystals; surface radical polymerization; epoxy; nanocomposites; fracture toughness

INTRODUCTION

Epoxy polymers are a class of important thermosets and they have widely been employed in a variety of fields owing to their excellent chemical resistance, high modulus and adhesive properties.^{1,2} However, epoxy thermosets are inherently brittle owing to their highly crosslinked structures. Therefore, successful application of epoxies requires improvement of toughness via structural modification. It is recognized that epoxies can be toughened by incorporating elastomers^{3–5} and thermoplastics.^{6,7} In these systems of modification, epoxy curing is generally started from the initial homogeneous mixtures composed of epoxy precursors and modifiers. As curing reactions proceed, the systems are gradually transformed into heterogeneous morphologies, namely reaction-induced phase separation (RIPS) occurs.^{8,9} In principle, there are two driving forces for RIPS. The first is the decrease in contribution of mixing entropy (ΔS_m) to mixing free energy (ΔG_m) during the curing process. The second is the alteration in inter-component interaction parameters (χ_{12}) since epoxy monomers are gradually transformed into crosslinked polymers with the occurrence of curing reactions. It is the formation of phase-separated morphologies that results in the improvement of fracture toughness. RIPS generally occurs on micrometer scales because the modifiers are homopolymers or random copolymers. Depending on the type of modifier (e.g. elastomers or thermoplastics), the materials can be toughened via several mechanisms such as shear band yielding,¹⁰ blunting of crack growth tips¹¹ and rupture of modifier phases.¹² It has been recognized that thermosets such as epoxies can be alternatively toughened via the formation of nanostructures in the materials. In 1997, Bates and

co-workers¹³ reported that incorporating amphiphilic block copolymers in epoxies would produce nanostructured epoxy thermosets. The formation of a nanostructure follows self-assembly^{13,14} or reaction-induced microphase separation,^{15,16} which are quite contingent on the miscibility of block copolymers with the epoxy matrix after and before curing reactions. More importantly, these nanostructured thermosets displayed enhanced fracture toughness.^{17,18}

Cellulose is one of the typical biopolymers with β -D-glucopyranosyls as the repeat units. Owing to some important features such as biodegradability, high mechanical strength and nontoxicity, cellulose has been applied in a variety of fields. Cellulose nanocrystals (CNCs) are made from natural cellulose, being of nanometric sizes.^{19–26} Owing to high ratios of length to diameter, CNCs are a type of ideal nanofiller for preparing nanocomposites with improved mechanical properties.^{27–30} Nonetheless, CNCs inherently are apt to agglomerate in epoxies owing to the high surface energy and specific area. It is a challenging task to achieve fine dispersions of CNCs in thermosetting polymers. To suppress the tendency of aggregation of CNCs, it is a requirement to form efficient chemical linkages between the surface of the CNCs and

* Correspondence to: L Li or S Zheng, Department of Polymer Science and Engineering and the State Key Laboratory of Metal Matrix Composites, Shanghai Jiao Tong University, Shanghai 200240, China. E-mail: lli_sjtu@163.com (Li); E-mail: szheng@sjtu.edu.cn (Zheng)

Department of Polymer Science and Engineering and the State Key Laboratory of Metal Matrix Composites, Shanghai Jiao Tong University, Shanghai, China

the epoxy matrix. In the past years, there have been several reports of the modification of epoxy thermosets with CNCs.^{31–43} In these previous works, CNCs were generally surface-functionalized via mercerization, oxidation, amination, acetylation and alkalization to introduce reactive or functional groups to improve the affinity of CNCs with epoxy matrix.^{44–49} In the meantime, there have been a few reports of the surface functionalization of CNCs with polymer chains; these polymer-grafted CNCs were then introduced into epoxies to afford nanocomposites.^{50–53} For instance, Zhao *et al.*⁵¹ reported the surface modification of CNCs via grafting reaction of polyethyleneimine; the amino groups of polyethyleneimine were utilized to generate chemical bonds between CNCs and epoxy matrix so that the macroscopic aggregation of CNCs in the epoxy matrix was suppressed. The mechanical strength as well as thermal conductivity of the modified thermosets were significantly improved. More recently, Luo *et al.*⁵⁰ reported that the surface of CNCs was first modified with hyperbranched polyglycerol. The hyperbranched polyglycerol was further reacted with 4,4-di(β -hydroxyethoxy)biphenyl and toluene-2,4-diisocyanate to afford hyperbranched polymers bearing many carbamate moieties to improve the compatibility (or/and reactivity) of the functionalized CNCs with epoxy. It was found that the epoxy composites containing such polymer-functionalized CNCs displayed improved tensile strength, impact strength and flexural modulus.

In this paper, we report a new functionalization of CNCs with poly(*N*-vinylpyrrolidone) (PVPy) via a surface living radical polymerization approach. Such PVPy-grafted CNCs (denoted CNC-PVPy) were then used as a modifier to toughen epoxy. Since PVPy is fully miscible with epoxy,⁵⁴ the PVPy chains grown from the surface of CNCs would act as a compatibilizer to facilitate the dispersion of CNCs in the epoxy. It should be pointed out that the dispersion of CNCs is based on the physical interaction of CNCs with epoxy. This strategy is in marked contrast to those reported in the literature^{51,52} in which the terminal groups of functionalized CNCs reacted with the precursors of epoxy to facilitate the dispersion of CNCs in epoxy. To the best of our knowledge, there has been no previous report in this regard. The purpose of this work was twofold. First, the surface-grafting polymerization of *N*-vinylpyrrolidone (NVP) was carried out to obtain CNC-PVPy. Second, the fracture toughness of nanocomposites of epoxy with CNC-PVPy was investigated to establish the correlation of the microstructure of the nanocomposites with mechanical properties.

EXPERIMENTAL

Materials

CNCs were purchased from ScienceK Co., China. According to the supplier, the CNCs were prepared through sulfuric acid hydrolysis of softwood pulp. A morphological observation by means of atomic force microscopy (AFM) showed that a single CNC crystal had an average length of $L = 150\text{--}230$ nm and a diameter of $D = 5\text{--}15$ nm. Diglycidyl ether of bisphenol A (DGEBA) was supplied by Shanghai Resin Co., China and the quoted epoxide value was 0.51. 4,4'-Methylenebis(2-chloroaniline) (MOCA) was obtained from Alfa Aesar Co., China. Isopropylxanthic disulfide (DIP) was purchased from Shanghai Yuanye Bio-Tech Co., China; it was purified by recrystallization from ethanol. NVP, 4,4'-azobis(4-cyanovaleic acid) (ACVA) and 2,2'-azobisisobutyronitrile (AIBN) were purchased from Adamas Reagent Co., China. AIBN was recrystallized from ethanol and NVP was passed through a

basic alumina column. The other reagents and solvents such as thionyl chloride, magnesium sulfate, 1,4-dioxane, triethylamine (TEA), toluene, tetrahydrofuran (THF), dichloromethane (DCM) and diethyl ether were supplied by Sinopharm Chemical Reagent Co., China.

Synthesis of chain transfer agent

DIP (80 g, 295.79 mmol), ACVA (128 g, 457.14 mmol) and 1,4-dioxane (500 mL) were added in a flask and the mixture was bubbled with highly pure nitrogen for 30 min. After that, the flask was transferred into an oil bath at 70 °C, and the reaction was allowed to proceed at this temperature for 24 h. After reaction, the majority of solvent was removed and the concentrated solution was added dropwise into petroleum ether. The precipitates were collected and dried *in vacuo* at 40 °C for 24 h. 4-Cyano-4-(isopropoxycarbonothioylthio)pentanoic acid (CIPA; 128.840 g) was obtained and the yield was 79.1%. ¹H NMR (CDCl₃; ppm): 5.83 (m, 1H, —OCH(CH₃)₂), 2.67 (t, 2H, HOOCCH₂CH₂—), 2.25–2.38 (m, 2H, HOOCCH₂—), 1.77 (s, 3H, —C(CN)CH₃), 1.52 (d, 6H, —OCH(CH₃)₂). ¹³C NMR (CDCl₃; ppm): 206.02 (—C—OCH(CH₃)₂), 177.22 (—COOH), 119.85 (—CN), 80.17 (—O—CH(CH₃)₂), 45.02 (—CHCH₃), 33.45 (—C(CN)CH₃), 29.32 (—CH₂CH₂COOH), 24.97 (—CH₂COOH), 21.07 (—O—CH(CH₃)₂).

Surface RAFT/MADIX polymerization of CNCs

First, CIPA (48 g, 0.175 mol) was dissolved in DCM (100 mL) and thionyl chloride (24 mL) was added dropwise to the solution. The reaction was allowed to proceed at 45 °C for 3 h. After reaction, the excess thionyl chloride was distilled off and the product was dissolved in anhydrous THF (100 mL). The solution was added dropwise into a THF/TEA suspension (400 mL of THF and 200 mL of TEA) of CNCs (12 g) at 0 °C. The reaction was performed at 45 °C for 24 h. After filtration, the solids were collected and washed with water three times. After drying, the product (CNC-CTA; 16.600 g) was obtained with a yield of 33.2%. FTIR (KBr window; cm⁻¹): 3600–3000 (O—H), 2910 (—CH—), 1731 (—COO—), 1161–1031 (C—O—C), 897 (β -glycosidic linkages).

Second, CNC-CTA (10 g), NVP (20 g, 179.95 mmol), AIBN (2 mg) and 1,4-dioxane (20 mL) were added into a 100 mL flask. The system was bubbled with highly pure nitrogen for 30 min. On heating to 75 °C, the polymerization was performed for 24 h. After polymerization, the mixture was added dropwise into diethyl ether (200 mL). The precipitates were collected and dried *in vacuo* at 40 °C for 24 h. The product (CNC-PVPy; 20.750 g) was obtained and the conversion of NVP was 53.75%. FTIR (KBr; cm⁻¹): 3600–3000 (O—H), 2910 (—CH—), 1731 (—COO—), 1660 (—C=O), 1161–1031 (C—O—C), 897 (β -glycosidic linkages).

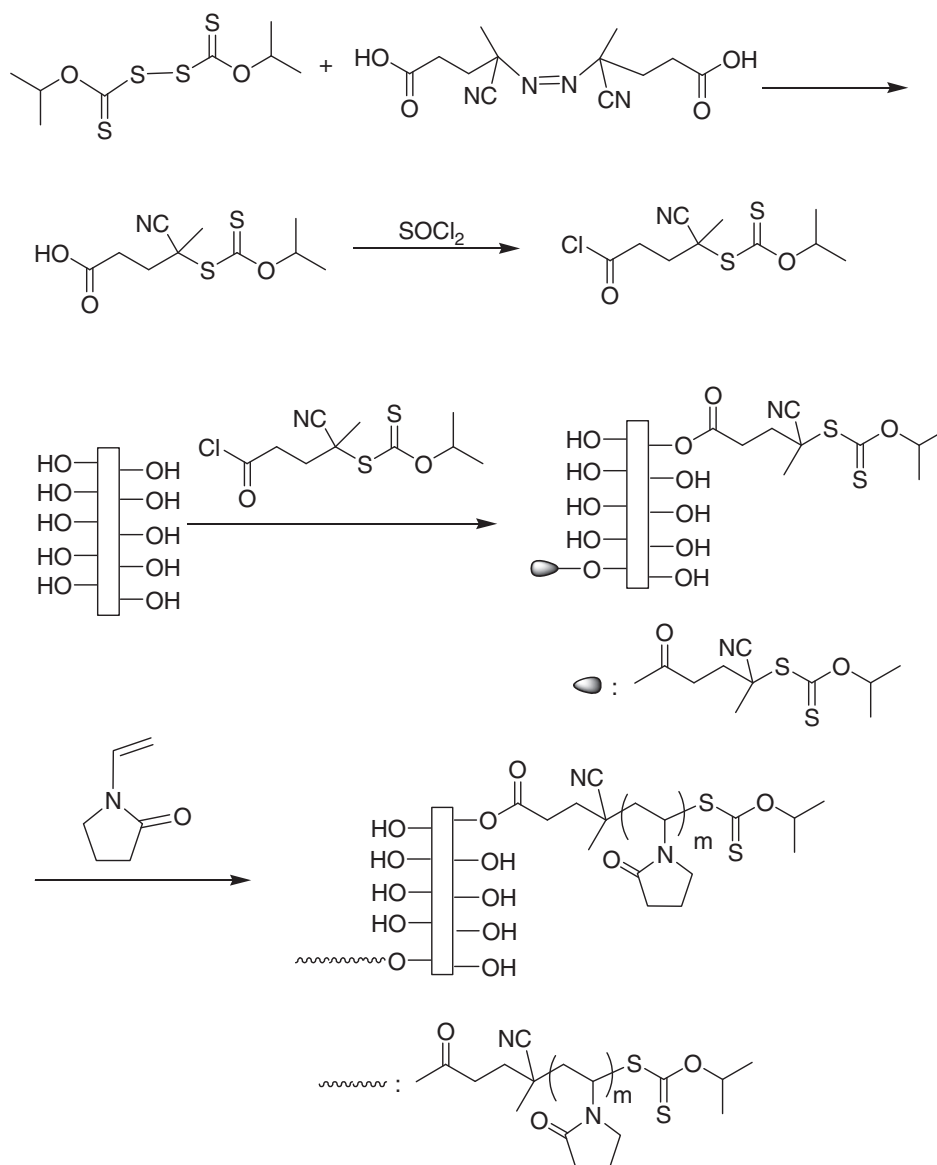
Preparation of nanocomposites of epoxy with CNCs

The desired amount of CNC-PVPy was added to DGEBA. On heating to 110 °C, stoichiometric MOCA with respect to DGEBA was added and the mixture was vigorously stirred. The mixture was transferred into a Teflon mold and the curing reaction was performed at 150 °C for 5 h. Composites of epoxy with CNC-PVPy were obtained with a mass fraction of CNC-PVPy up to 40 wt%.

RESULTS AND DISCUSSION

Synthesis of CNC-PVPy

The synthesis route for CNC-PVPy is shown in Scheme 1. First, the surface of CNCs was functionalized with xanthate via a surface esterification reaction of CNCs with 4-cyano-4-(isopropoxycarbonothioylthio)



Scheme 1. Functionalization of CNCs and synthesis of PVPy-grafted CNCs.

pentanoic chloride. The latter was obtained via the reaction of CIPA with thionyl chloride. Herein, CIPA was synthesized via the atom transfer radical reaction of DIP with ACVA. Second, CNC-PVPy was synthesized with the xanthate-functionalized CNCs as chain transfer agent. The successful synthesis of CIPA was confirmed by means of NMR spectroscopy. Figure S1 (Appendix S1) shows the ¹H NMR and ¹³C NMR spectra of CIPA. The peak at 5.83 ppm was assignable to the methine protons whereas those at 2.67 and 2.31 ppm were assignable to the protons of methylene groups. The peaks at 1.77 and 1.52 ppm were assignable to protons of the methyl groups connected to quaternary and tertiary carbon, respectively. In the ¹³C NMR spectrum, the signals at 206.02, 177.22 and 119.85 ppm are assigned to the carbon nuclei of carbonyl, cyano and the carbon connected to sulfur atom, respectively. The signals at 80.17, 33.45, 29.32, 24.97 and 21.07 ppm are assigned to the tertiary, quaternary, secondary and primary carbon nuclei, respectively. Notably, a new peak at 45.02 ppm appeared, which could result from the rearrangement of atom transfer radical reaction products. It is proposed that the new resonance is attributable to the nucleus of tertiary carbon in 4-cyanovaleric moiety after

a cyan group was lost in the reaction of arrangement. A similar phenomenon was found in the products of reaction of DIP with AIBN.⁵⁵

The functionalization of CNCs with xanthate and/or PVPy chains was readily confirmed with solubility tests and by the use of Fourier transform infrared (FTIR) spectroscopy. The pristine CNCs were highly hydrophilic and readily dispersed in water due to the existence of a great number of hydroxyl groups at the surface (Fig. 1(A)). After reacting with 4-cyano-4-(isopropoxycarbonylthio)pentanoic chloride, the product was poorly dispersed in aqueous media (Fig. 1(B)) since many of the surface hydroxyl groups were esterified into xanthate moieties, i.e. CNC-CTA was obtained. However, the solubility was further improved after water-soluble polymer chains (i.e. PVPy) were grafted from these xanthate sites via reversible addition-fragmentation chain transfer/macromolecular design via interchange of xanthates (RAFT/MADIX) polymerization (Fig. 1(C)). The surface-functionalized CNCs were subjected to FTIR spectroscopy (Fig. S2, Appendix S1). For pristine CNCs, the strong band at 3400 cm⁻¹ is assignable to the stretching vibration of hydroxyl

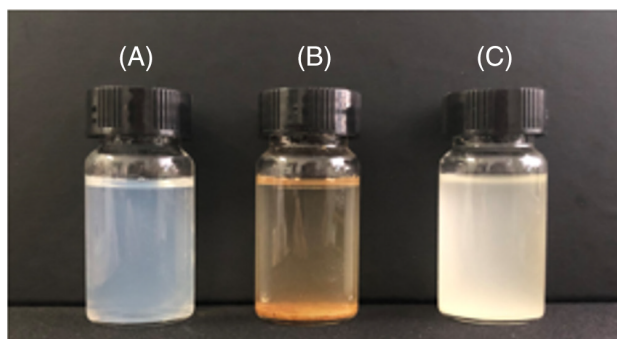
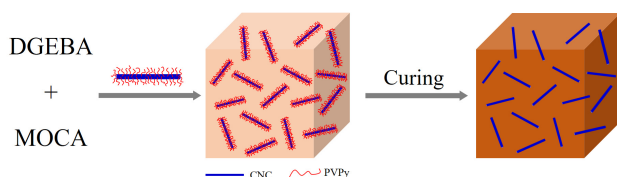


Figure 1. Suspensions of (A) CNCs, (B) CNC-CTA and (C) CNC-PVPy in water.



Scheme 2. Formation of nanocomposites of epoxy with CNCs.

groups. The band centered at $\approx 1100\text{ cm}^{-1}$ is attributable to the stretching vibration of ether bond (C—O—C linkage)²⁷ and that at 893 cm^{-1} is assigned to β -glucosidic linkage.³³ On esterification with 4-cyano-4-(isopropoxycarbonothioylthio)pentanoic chloride, a shoulder band at 1731 cm^{-1} appeared, attributable to the stretching vibration of ester carbonyl groups. This result revealed that the esterification had been successfully carried out. After the RAFT/MADIX polymerization, a strong band at 1660 cm^{-1} appeared, which was assignable to carbonyl groups of pyrrolidone rings. To determine the mass fraction of PVPy chains in CNC-PVPy, the sample was used for elemental analysis. The overall content of nitrogen element was measured to be 6.55 wt%. By using the content of nitrogen element, the mass fraction of PVPy chains was calculated to be 51.9 wt%.

Nanocomposites of epoxy with CNC-PVPy

CNC-PVPy obtained as described above was incorporated into epoxy to prepare the nanocomposites (Scheme 2.). Notably, CNC-PVPy was readily dispersed in the precursors of epoxy thermoset (i.e. DGEBA + MOCA), which was in sharp contrast to the case of the pristine CNCs. The improvement in dispersion is attributable to the grafting of PVPy onto the surfaces of CNCs. It is proposed that the grafted PVPy chains acted as a compatibilizer for the blends of CNCs with epoxy precursors. After curing, the thermosets were homogeneous and no macroscopic aggregation of CNCs was observed, implying that the CNCs were well dispersed into the thermosetting matrices of epoxy (Fig. 2). For comparison, we also prepared a composite of epoxy with 9.62 wt% of pristine CNCs; the mass fraction of CNCs was controlled to equal that in the composite of epoxy with 20 wt% of CNC-PVPy. It is noted that the composite of epoxy with pristine CNCs was heterogeneous, and the CNCs were precipitated at one side of the sample (Fig. 2). In contrast, all the composites of epoxy with CNC-PVPy were homogeneous and transparent. This result indicates that the PVPy chains grafted onto the surface of CNCs can efficiently act as a compatibilizer to facilitate the dispersion of CNCs in epoxy.

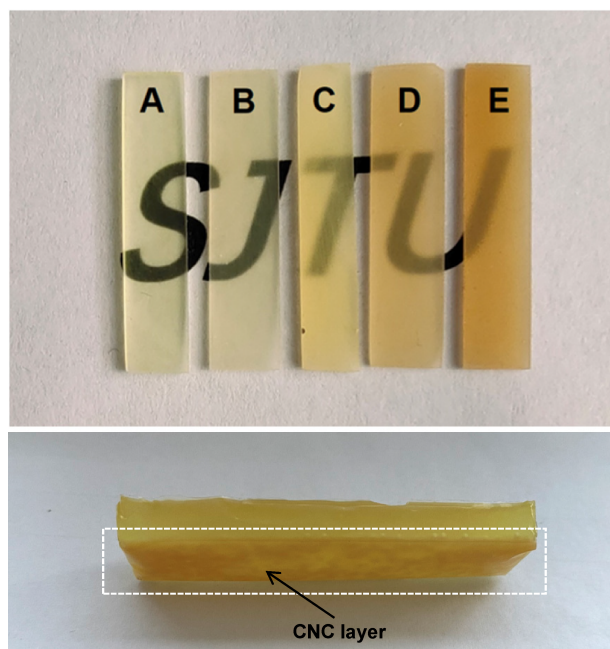


Figure 2. Photographs of: (A) plain epoxy and nanocomposites containing (B) 10, (C) 20, (D) 30 and (E) 40 wt% of CNC-PVPy (top); and cured blend of epoxy with 9.62 wt% of pristine CNCs (bottom).

To examine the crystallization behavior of CNCs in the epoxy, XRD measurements were performed. Figure 3 shows the XRD curves of the pristine CNCs and the nanocomposite containing 40 wt% of CNC-PVPy. For pristine CNCs, there were four diffraction peaks at $2\theta = 14.7^\circ, 16.4^\circ, 22.6^\circ$ and 35.2° , assignable to reflections of (10 $\bar{1}$), (101), (002) and (040) planes, respectively. The crystallization index (X_c) of the pristine CNCs can be calculated using the following equation^{56,57}:

$$X_c = \frac{A_c}{A_c + A_a} \times 100\% \quad (1)$$

where A_c is the integral area of the crystalline component and A_a is the integral area of the amorphous component. For the nanocomposite, these diffraction peaks were still discernable but their intensity was significantly decreased. The XRD results revealed that the crystal structure of CNCs did not change, namely cellulose still existed in the form of microcrystals. The morphologies of the composites of epoxy with CNCs were observed using AFM. Before the measurements, the samples were sliced using an ultrathin microtome and the sections were used for morphological observations. For comparison, the morphology of CNCs was also observed using AFM. Figure 4 shows the AFM image of pristine CNCs. It is seen that the average length and diameter of a single CNC were 150–230 and 5–15 nm, respectively. Figure 5 shows the AFM images of nanocomposites containing 20 and 40 wt% of CNC-PVPy. Inhomogeneous morphologies at the nanometric scale were obtained for the samples. Notably, the fibrous nano-objects were uniformly dispersed in the continuous matrices. In terms of the difference in viscoelasticity between the CNCs and epoxy matrix, the fibrous nano-objects are attributable to CNCs and the continuous matrix to epoxy. The CNCs were dispersed into the epoxy matrix in the form of single nano-objects. The fact that no macroscopic aggregates of CNCs were formed indicated

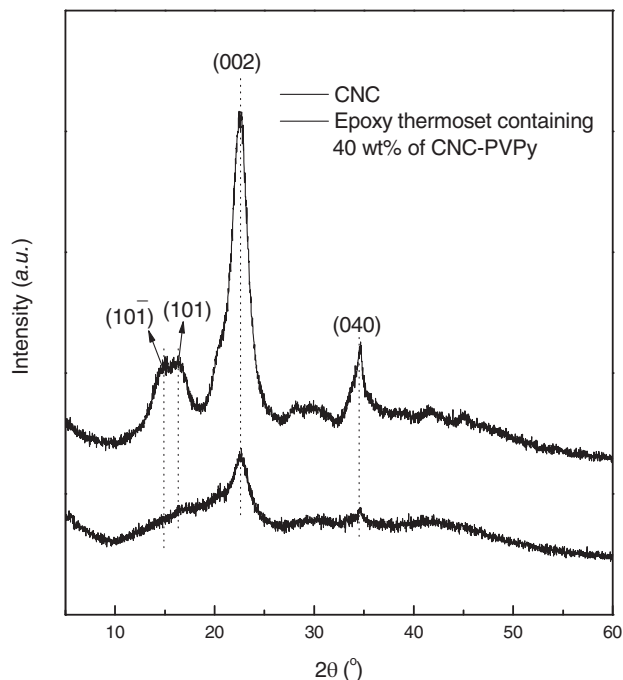


Figure 3. XRD curves of pristine CNCs and nanocomposite containing 40 wt% of CNC-PVPy.

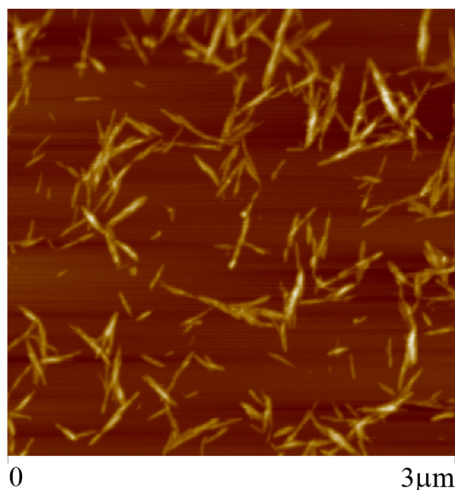


Figure 4. AFM image of pristine CNCs.

that the PVPy chains on the surface of the CNCs were capable of compatibilizing the thermosetting blends of epoxy with CNC. This judgment was further confirmed using dynamic mechanical thermal analysis (DMTA).

Figure 6 shows the DMTA curves of plain epoxy and the nanocomposites. For the plain epoxy, a major peak at 159 °C was displayed in the plot of $\tan \delta$ versus temperature, which was assignable to the glass transition of the thermoset. In addition, there were two secondary transitions at ca 75 and -65 °C, respectively. The former (denoted $T_{\beta 1}$) is attributable to diphenylmethane structural units ($-\text{C}_6\text{H}_4-\text{C}(\text{CH}_3)_2-\text{C}_6\text{H}_4-$) whereas the latter (denoted $T_{\beta 2}$) to hydroxyether linkages ($-\text{O}-\text{CH}_2-\text{CH}(\text{OH})-\text{CH}_2-\text{O}-$) in the epoxy backbone. Upon introducing CNC-PVPy, notably, the glass transition temperature (T_g) shifted to

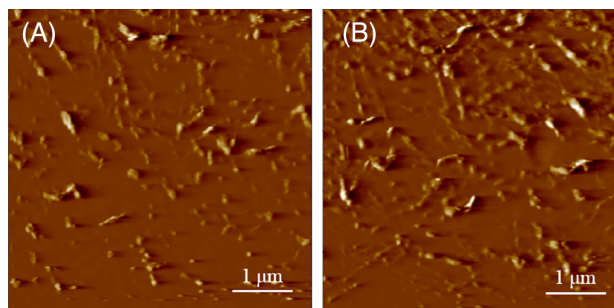


Figure 5. AFM images of nanocomposites containing (A) 20 and (B) 40 wt% of CNC-PVPy.

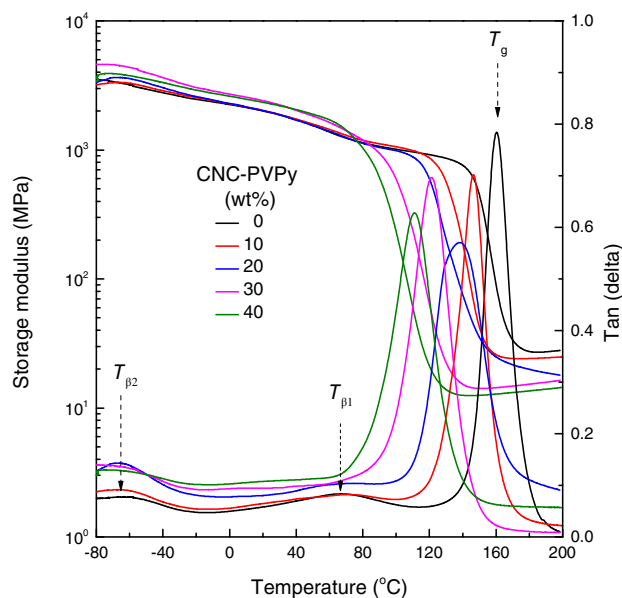


Figure 6. Storage modulus and $\tan \delta$ of control epoxy and the nanocomposites as a function of temperature from DMTA measurements.

lower values. For the nanocomposite containing 40 wt% of CNC-PVPy, T_g was decreased to 111 °C. A similar phenomenon of a shift to lower temperature was also found for the secondary transitions ($T_{\beta 1}$ and $T_{\beta 2}$). This phenomenon can be explained on the basis of the intimate mixing of the epoxy network with the PVPy chains grafted from the surface of CNCs. In other words, the epoxy network was plasticized by a lower- T_g component (i.e. PVPy). The speculation that the PVPy chains grafted from the surface of CNCs had a lower T_g is readily confirmed using DSC. Figure 7 shows the DSC curves of control epoxy and CNC-PVPy. In both cases, single T_g values were exhibited. For CNC-PVPy, the single T_g is only ascribed to PVPy chains since CNCs are highly crystalline or T_g was too high to be detected. T_g of the PVPy chains was measured to be only 97 °C, which was significantly lower than that of the control epoxy (i.e. 141 °C). The glass transition behavior indicates that the PVPy chains grafted from the surface of CNCs intimately mixed with the epoxy network on the segmental scale. The complete miscibility of epoxy with PVPy is attributed to the intermolecular hydrogen bonding interactions between hydroxyl groups of epoxy matrix and carbonyl groups of PVPy.⁵⁴ It is this full miscibility that suppresses the aggregation of CNCs in the epoxy matrix, namely the nanocomposites were successfully obtained. In the nanocomposites, the fine dispersion of CNCs would significantly

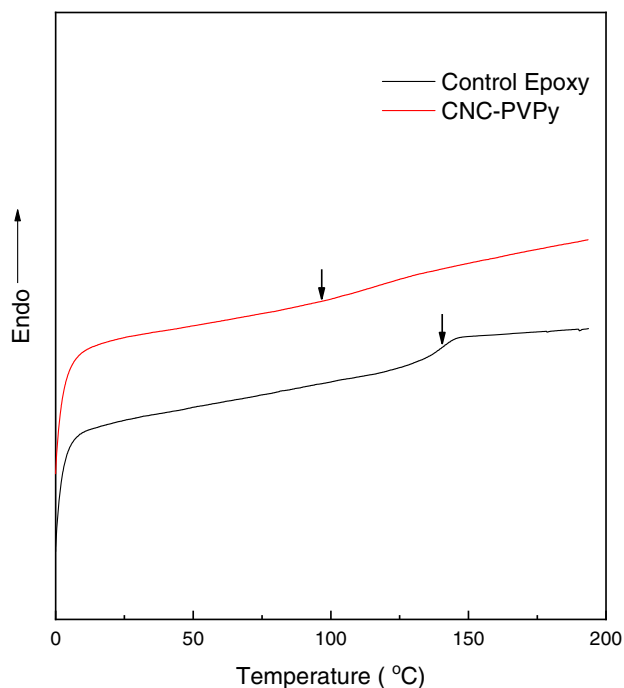


Figure 7. DSC curves of control epoxy and CNC-PVPy.

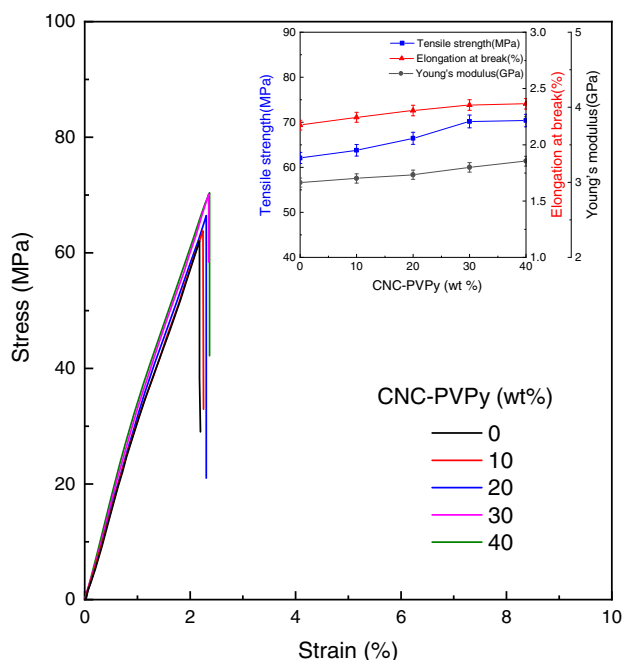


Figure 8. Strain–stress curves of control epoxy and nanocomposites.

reinforce the epoxy matrix, which was readily proved by the enhancement in modulus of the materials. From Fig. 6, the storage moduli of the nanocomposites in the glass states were much higher than that of the control epoxy. The higher the mass fractions of CNC-PVPy, the higher are the storage moduli of the nanocomposites. The enhanced storage moduli resulted from the nanoreinforcement effect of the CNCs on the epoxy matrix, which can be further evidenced with mechanical tests.

The mechanical properties of the nanocomposites were investigated by tensile measurements. Figure 8 shows the strain–stress

Table 1. Mechanical parameters of nanocomposites of epoxy and CNC-PVPy

CNC-PVPy (wt%)	Tensile strength (MPa)	Young's modulus (GPa)	Elongation at break (%)
0	62.07 ± 2.18	2.99 ± 0.05	2.17 ± 0.04
10	63.79 ± 2.45	3.05 ± 0.06	2.25 ± 0.03
20	66.43 ± 2.30	3.10 ± 0.06	2.31 ± 0.04
30	70.19 ± 2.35	3.21 ± 0.05	2.34 ± 0.05
40	70.39 ± 2.36	3.28 ± 0.07	2.37 ± 0.05

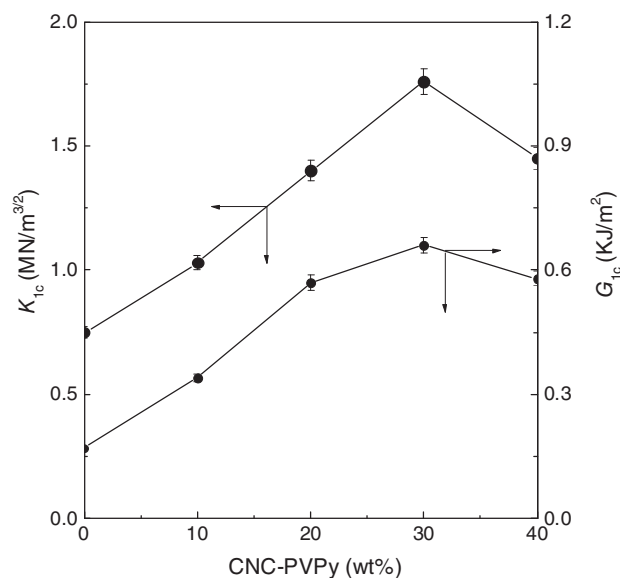


Figure 9. Plots of critical stress intensity factor (K_{1c}) and fracture energies (G_{1c}) of control epoxy and nanocomposites as a function of mass fraction of CNC-PVPy.

curves of control epoxy and the nanocomposites at a loading rate of 50 mm min^{-1} . The mechanical properties of the nanocomposites are also summarized in Table 1. All the samples displayed the behavior of brittle fracture. For the control epoxy, the tensile strength, elongation at break and Young's modulus were 62.07 MPa, 2.18% and 3.0 GPa, respectively. Upon introducing CNC-PVPy, the mechanical properties were slightly enhanced. When the mass fraction of CNC-PVPy was 40 wt%, the tensile strength, elongation at break and Young's modulus increased to 70.39 MPa, 2.38% and 3.28 GPa, respectively. The increased Young's moduli are assignable to the nanoreinforcement of CNCs. The increased tensile strength is a result of the introductions of fibrous nano-objects (i.e. CNCs) which had much stronger interactions with the epoxy matrix. The enhanced interactions between CNCs and epoxy resulted from the full miscibility of PVPy chains which were grafted from the surface of the CNCs. The increased elongation at break suggests that the ductility of the epoxy matrices of the nanocomposites was significantly increased owing to the intimate mixing of PVPy chains with the epoxy network. This finding was further corroborated by the toughening improvement of the nanocomposites compared to control epoxy.

Toughening of epoxy thermostets

To investigate the fracture toughness, control epoxy and the nanocomposites were subjected to three-point bending tests to

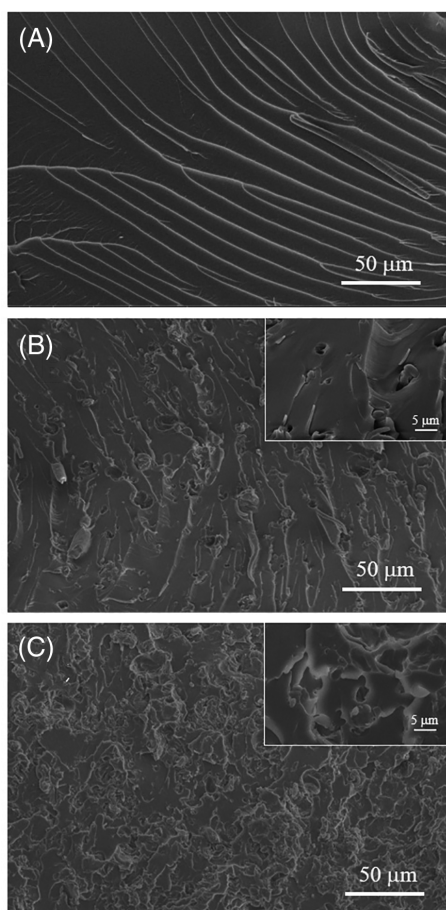


Figure 10. Field emission SEM images of tensile fracture surface of (A) control epoxy and nanocomposites containing (B) 20 wt% and (C) 40 wt% of CNC-PVPy.

measure their critical stress intensity factors (K_{1C}) and critical fracture energy (G_{1C}) (Scheme S1, Appendix S1). The plots of K_{1C} and G_{1C} as functions of the mass fraction of CNC-PVPy are shown in Fig. 9. For the control epoxy, the value of K_{1C} was measured to be $0.75 \text{ MN m}^{-3/2}$. Notably, all the nanocomposites displayed increased K_{1C} , indicating that the introduction of CNC-PVPy resulted in a significant improvement in fracture toughness. Notably, the nanocomposite containing 30 wt% of CNC-PVPy displayed the maximum in K_{1C} (i.e. $K_{1C} = 1.76 \text{ MN m}^{-3/2}$), which was 2.35 times that of the control epoxy. According to the values of K_{1C} and flexural moduli (E), the fracture energy release rates (G_{1C}) were calculated, as also shown in Fig. 9. The K_{1C} and G_{1C} results indicate that the toughness of epoxy has been significantly improved with the incorporation of CNCs. The toughening effect was also evidenced with the change in surface morphologies of fracture ends of the samples. The fracture ends from the mechanical tests described above were used for morphological observation using field emission SEM. Figure 10 shows the SEM micrographs of control epoxy and nanocomposites containing 20 and 40 wt% of CNC-PVPy. For the control epoxy, a great number of cracks were generated at the fracture surfaces and these cracks were parallel with each other, suggesting that the cracks were easily developed and that the growth of these cracks was less hindered. This behavior is indicative of brittle fracture of thermosets. However, for the nanocomposites, there were fewer cracks at the fracture surface. Furthermore, the growth directions

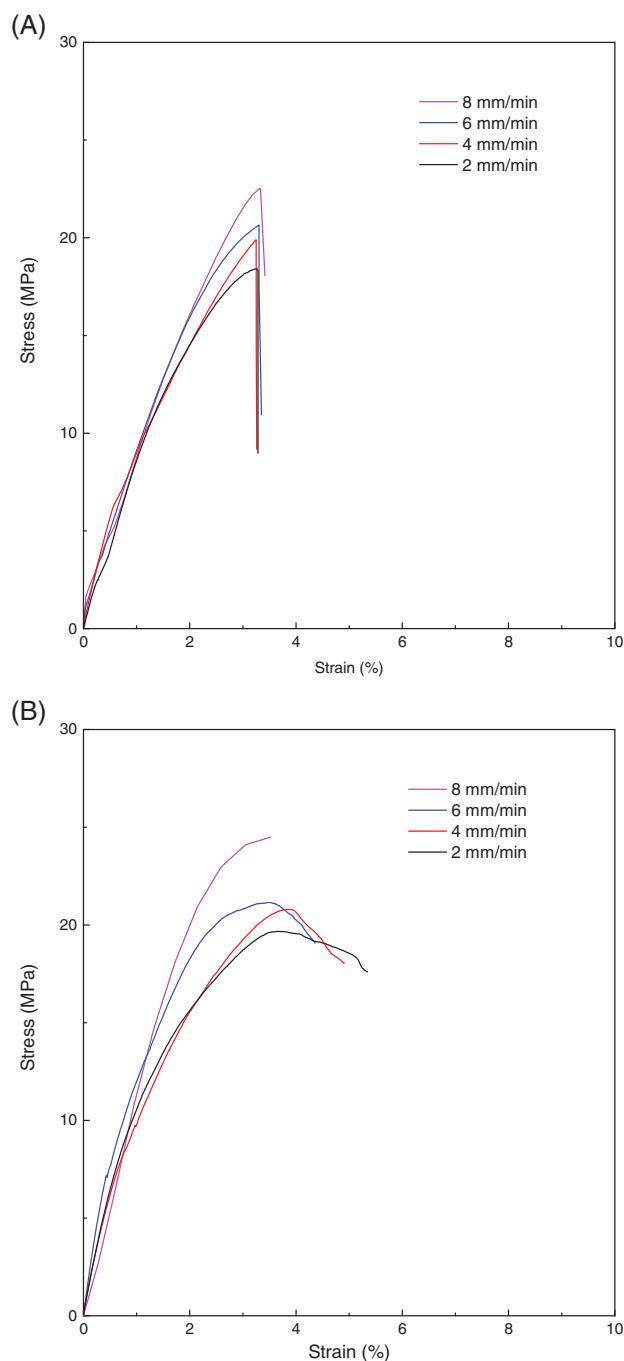


Figure 11. Strain-stress curves of (A) control epoxy and (B) nanocomposite containing 40 wt% of CNC-PVPy at variable loading rates.

of cracks were easily changed, which is typical of tough fracture behavior of thermosets. Notably, when the mass fraction of CNC-PVPy was 40 wt%, the parallel cracks were almost invisible, and the growth direction of the cracks were random. The morphologies of fracture ends indicate that the epoxy thermoset was indeed toughened with the introduction of CNCs.

For the nanocomposites of epoxy with CNCs, the improvement of toughness is attributable to: (i) the formation of nanostructured thermosets (i.e. CNCs were finely dispersed in the epoxy matrix) and (ii) the introduction of rigid and fibrous nanoreinforcement

(i.e. CNCs). Various researchers^{58–60} have investigated the toughening mechanisms in nanostructured thermosets containing block copolymers. It was found that depending on the viscoelasticity of nanodomains dispersed in continuous thermosetting matrices, debonding, nanocavitation and plastic deformation of thermosetting matrix around the nanodomains would be involved in the toughness improvement of thermosets. In the present case, the nanofillers (i.e. CNCs) were quite rigid and thus nanocavitation could not be a major toughening mechanism due to the inability of CNCs to deform. In addition, interfacial debonding of CNCs from the thermosetting matrix was not expected since CNCs had quite strong adhesion to the epoxy matrix through the strong hydrogen bonding between PVPy chains and the epoxy networks.⁶¹ The introduction of CNCs would disrupt the continuity of epoxy the network in the vicinity of CNC microdomains and could lead to the initiation of matrix shear yielding. It is proposed that the short PVPy chains on the surface of CNCs having a lower T_g (ca 97 °C) increased the segmental mobility of the epoxy matrix, which would result in the shear yielding of the matrix around CNC microdomains. To confirm the possible toughening mechanisms, we investigated the stress–strain behavior of control epoxy and the nanocomposites. Figure 11 shows the stress–strain curves of control epoxy and the nanocomposite containing 40 wt% of CNC-PVPy at variable loading rates. For the control epoxy, no yield points were exhibited in the stress–strain curves although the stretching rate was reduced as low as 2 mm min⁻¹, indicating that the sample was inherently brittle, i.e. the fracture was in a brittle manner. In marked contrast to this observation, there were clear yield points in the stress–strain curves of the nanocomposite. The appearance of yield points indicates that there was a behavior of plastic deformation of the thermosetting matrix in the tensile tests, i.e. the sample displayed the behavior of tough fracture. The stress–strain results suggest that there was indeed a yielding behavior of matrix deformation. It should be pointed out that the toughness improvement could be additionally ascribed to the blunting behavior of crack growth tips by the fibrous nano-objects (i.e. CNCs).^{62, 63}

CONCLUSIONS

CNCs were functionalized via surface-initiated RAFT/MADIX polymerization. The pristine CNCs were first treated with 4-cyano-4-(isopropoxycarbonothioylthio) pentanoic chloride and the resulting xanthate-functionalized CNCs were used to mediate the radical polymerization of NVP. CNC-PVPy was successfully obtained with a mass fraction of PVPy of 51.9 wt%. It was found that CNC-PVPy can be well dispersed into epoxy thermosets, i.e. nanocomposites of epoxy with CNCs were successfully obtained. The fine dispersion of CNCs in the epoxy matrix is responsible for the intimate mixing of PVPy chains with epoxy networks. Results of mechanical tests indicate that epoxy thermosets can be significantly toughened with the introduction of CNCs with a dispersion in the form of single fibrous nano-objects. The toughening of epoxy thermosets is mainly attributed to the plastic deformation of the epoxy matrix which was initiated with the fine dispersion of CNCs.

ACKNOWLEDGEMENT

The authors thank the National Natural Science Foundation of China (grant nos. 21774078, 51973113 and 51133003) for financial support.

SUPPORTING INFORMATION

Supporting information may be found in the online version of this article.

REFERENCES

- 1 Ellis B, *Chemistry and Technology of Epoxy Resins*. Springer, Dordrecht (1993).
- 2 Parameswaranpillai J, Hameed N, Pionteck J and Woo NM, *Handbook of Epoxy Blends*. Springer, Cham (2017).
- 3 Ramos VD, da Costa HM, VLP S and RSV N, *Polym Test* **24**:387–394 (2005).
- 4 Chikhi N, Fellahi S and Bakar M, *Eur Polym J* **38**:251–264 (2002).
- 5 Ochi M, Morishita T, Kokufu S and Harada M, *Polymer* **42**:9687–9695 (2001).
- 6 Hourston DJ and Lane JM, *Polymer* **33**:1379–1383 (1992).
- 7 Huang P, Zheng S, Huang J, Guo Q and Zhu W, *Polymer* **38**:5565–5571 (1997).
- 8 Pearson RA and Yee AF, *J Mater Sci* **24**:2571–2580 (1989).
- 9 Riew CK and Kinloch AJ, *Toughened Plastics I: Science and Engineering*. American Chemical Society, Washington, DC (1993).
- 10 Gilbert A and Bucknall C, *Epoxy Resin Toughened with Thermoplastic*. Wiley, Amsterdam (1991).
- 11 Iijima T, Tomoi M, Tochimoto T and Kakiuchi H, *J Appl Polym Sci* **43**:463–474 (1991).
- 12 Liu J, Thompson ZJ, Sue HJ, Bates FS, Hillmyer MA, Hillmyer MA et al., *Macromolecules* **43**:7238–7243 (2010).
- 13 Hillmyer MA, Lipic PM, Hajduk DA, Almdal K and Bates FS, *J Am Chem Soc* **119**:2749–2750 (1997).
- 14 Lipic PM, Bates FS and Hillmyer MA, *J Am Chem Soc* **120**:8963–8970 (1998).
- 15 Meng F, Zheng S, Li H, Liang Q and Liu T, *Macromolecules* **39**:5072–5080 (2006).
- 16 Meng F, Zheng S, Zhang W, Li H and Liang Q, *Macromolecules* **39**:711–719 (2006).
- 17 Yang X, Yi F, Xin Z and Zheng S, *Polymer* **50**:4089–4100 (2009).
- 18 Ding H, Zhao B, Mei H, Li L and Zheng S, *Polym Eng Sci* **59**:2387–2396 (2019).
- 19 Kloser E and Gray DG, *Langmuir* **26**:13450–13456 (2010).
- 20 de Castro DO, Bras J, Gandini A and Belgacem N, *Carbohydr Polym* **137**:1–8 (2016).
- 21 Wohlhauser S, Delepierre G, Labet M, Morandi G, Thielemans W, Weder C et al., *Macromolecules* **51**:6157–6189 (2018).
- 22 Fatona A, Berry RM, Brook MA and Moran-Mirabal JM, *Chem Mater* **30**:2424–2435 (2018).
- 23 Habibi Y, Goffin AL, Schiltz N, Duquesne E, Dubois P and Dufresne A, *J Mater Chem* **18**:5002–5010 (2008).
- 24 Boujemaoui A, Cobo Sanchez C, Engstroem J, Bruce C, Fogelstroem L, Carlmark A et al., *ACS Appl Mater Interfaces* **9**:35305–35318 (2017).
- 25 Cao X, Habibi Y and Lucia LA, *J Mater Chem* **19**:7137–7145 (2009).
- 26 Zoppe JO, Peresin MS, Habibi Y, Venditti RA and Rojas O, *ACS Appl Mater Interfaces* **1**:1996–2004 (2009).
- 27 Xu S, Girouard N, Schueneman G, Shofner ML and Meredith JC, *Polymer* **54**:6589–6598 (2013).
- 28 Cai S, Li Y, Liu H and Mai Y, *Compos Sci Technol* **181**:107673 (2019).
- 29 Asadi A, Miller M, Moon R and Kalaitzidou K, *Express Polym Lett* **10**:587–597 (2016).
- 30 Boujemaoui A, Mazières S, Malmström E, Destarac M and Carlmark A, *Polymer* **99**:240–249 (2016).
- 31 Neves RM, Ornaghi HL Jr, Zattera AJ and Amico SC, *Carbohydr Polym* **255**:117366 (2021).
- 32 Nair SS, Dartailh C, Levin DB and Yan N, *Polymers* **11**:612 (2019).
- 33 Trinh BM and Mekonnen T, *Polymer* **155**:64–74 (2018).
- 34 Yin Y, Ma J, Tian X, Jiang X, Wang H and Gao W, *Cellulose* **25**:6447–6463 (2018).
- 35 Yue L, Maiorana A, Khelifa F, Patel A, Raquez JM, Bonnaud L et al., *Polymer* **134**:155–162 (2018).
- 36 Saba N, Safwan A, Sanyang M, Mohammad F, Pervaiz M, Jawaid M et al., *Int J Biol Macromol* **102**:822–828 (2017).
- 37 Abraham E, Kam D, Nevo Y, Slattegard R, Rivkin A, Lapidot S et al., *ACS Appl Mater Interfaces* **8**:28086–28095 (2016).
- 38 Girouard N, Schueneman GT, Shofner ML and Meredith JC, *Polymer* **68**:111–121 (2015).

- 39 Panchal P and Mekonnen TH, *Nanoscale Adv* **1**:2612–2623 (2019).
- 40 Seok H and Kim DS, *Polym Eng* **60**:439–445 (2020).
- 41 Pruksawan S, Samitsu S, Fujii Y, Torikai N and Naito M, *ACS Appl Mater Interfaces* **2**:1234–1243 (2020).
- 42 Peng SX, Shrestha S, Yoo Y and Youngblood JP, *Polymer* **112**:359–368 (2017).
- 43 Aziz T, Fan H, Zhang X and Khan FU, *Mater Res Express* **6**:1150–1157 (2019).
- 44 Le Hoang S, Vu CM, Pham LT and Choi HJ, *Polym Bull* **75**:2607–2625 (2018).
- 45 Kalali EN, Hu Y, Wang X, Song L and Xing W, *Ind Crop Prod* **129**:434–439 (2019).
- 46 Isogai A, Saito T and Fukuzumi H, *Nanoscale* **3**:71–85 (2011).
- 47 Zhang M, Li M, Liu L, Fu J, Jin L, Shang L et al., *Polym Compos* **40**:744–752 (2019).
- 48 Shrestha S, Chowdhury RA, Toomey MD, Betancourt D, Montes F and Youngblood JP, *Cellulose* **26**:9631–9643 (2019).
- 49 Qiu B, Li M, Zhang X, Chen Y, Zhou S, Liang M et al., *Mater Chem Phys* **258**:123677 (2021).
- 50 Luo Q, Li Y, Ren L, Xu X and Lu S, *Polymers* **10**:1024 (2018).
- 51 Zhao J, Li Q, Zhang X, Xiao M, Zhang W and Lu C, *Carbohydr Polym* **157**:1419–1425 (2017).
- 52 Luo Q, Li Y, Pan L, Song L, Yang J, Wu L et al., *J Mater Sci* **51**:8888–8899 (2016).
- 53 Xiao X, Lu S, Pan L, Zeng C, He Z, Gao J et al., *J Polym Res* **23**:72–81 (2016).
- 54 Xiang Y, Li L and Zheng S, *Polymer* **98**:344–352 (2016).
- 55 Zhang C, Li L, Cong H and Zheng S, *J Polym Sci Part A* **52**:952–962 (2014).
- 56 Lu P and Hsieh Y, *Carbohydr Polym* **87**:564–573 (2012).
- 57 Johan Foster E, Moon RJ, Agarwal UP, Bortner MJ, Bras J, Camarero-Espinosa S et al., *Chem Soc Rev* **47**:2609–2679 (2018).
- 58 Dean JM, Grubbs RB, Saad W, Cook RF and Bates FS, *J Polym Sci Part B* **41**:2444–2456 (2003).
- 59 Liu J, Sue H, Thompson ZJ, Bates FS, Dettloff M, Jacob G et al., *Acta Mater* **57**:2691–2701 (2009).
- 60 Dean JM, Lipic PM, Grubbs RB, Cook RF and Bates FS, *J Polym Sci Part B* **39**:2996–3010 (2001).
- 61 Declet-Perez C, Francis LF and Bates FS, *ACS Macro Lett* **2**:939–943 (2013).
- 62 Jajam KC, Tippur HV and Int J, *Solid Struct* **49**:1127–1146 (2012).
- 63 Wong KJ, Zahi S, Low KO and Lim CC, *Mater Des* **31**:4147–4154 (2010).